Available online at www.sciencedirect.com
ScienceDirect
Trans. Nonferrous Met. Soc. China 30(2020) 3367−3378
Transactions of Nonferrous Metals Society of China
www.tnmsc.cn

Recovery of zinc and lead from Yahyali non-sulphide flotation tailing by sequential acidic and sodium hydroxide leaching in the presence of potassium sodium tartrate

Sait KURSUNOGLU[1], Soner TOP[1], Muammer KAYA[2]

1. Department of Materials Science & Nanotechnology Engineering, Abdullah Gul University, Kayseri 38100, Turkey;
2. Division of Mineral Processing, Department of Mining Engineering,
Eskisehir Osmangazi University, Eskisehir 26480, Turkey

Received 3 April 2020; accepted 4 September 2020

Abstract: The recovery of zinc and lead from Yahyali non-sulphide flotation tailing using sulfuric acid followed by sodium hydroxide leaching in the presence of potassium sodium tartrate was experimentally investigated. In the acidic leaching stage, the effects of pH, solid-to-liquid ratio and temperature on the dissolution of zinc from the tailing were explored. 82.3% Zn dissolution was achieved at a pH of 2, a temperature of 40 °C, a solid-to-liquid ratio of 20% and a leaching time of 2 h, whereas the iron and lead dissolutions were determined to be less than 0.5%. The sulfuric acid consumption was found to be 110.6 kg/t (dry tailing). The leaching temperature had no beneficial effect on the dissolution of zinc from the tailing. The acidic leach solution was subjected to an electrowinning test. The cathode product consisted of 99.8% Zn and 0.15% Fe. In the alkaline leaching stage, the Pb dissolution increased slightly in the presence of potassium sodium tartrate. More than 60% of Pb was taken into the leach solution when the leaching temperature increased from 40 to 80 °C. The final leach residue was analyzed by XRD and XRF. The XRD results indicated that the major peaks originated from the goethite and quartz while minor peaks stem from smithsonite and cerussite. The XRF analysis demonstrated that the residue contained 70.3% iron oxide. Based on the sequential leaching experiments, the zinc and lead were excellently depleted from the flotation tailing, leaving a considerable amount of iron in the final residue.

Key words: zinc; lead; flotation tailing; sequential leach

1 Introduction

Zinc and lead are the most used non-ferrous base metals in the world after copper and aluminum. It is, however, estimated that around 26.36% and 24.39% of the mined zinc and lead, respectively, are lost in the processing activities and the mineral beneficiation process, which is commonly achieved via flotation, representing 50.67% and 45.51% of the losses [1]. It is, therefore, estimated for the average of 12.6 million tons and 4.6 million tons of the annual mined zinc and lead, respectively, in the last decade, that about 1.7 million tons of zinc and 0.5 million tons of lead were ended up in the flotation tailing each year [2,3]. The processing of zinc and lead flotation tailing as a secondary resource for the two metals is therefore attractive not only from an environmental perspective to minimize the environmental impact of the mining activities but also from the economic perspective given the relative abundance of the resource which does not require mining cost.

There are millions of tonnes of lead−zinc sulphide ores treated by flotation techniques in metallurgical industries, which contain substantial amounts of non-ferrous and precious metal losses. Currently, metallurgical tailings can be considered

Corresponding author: Sait KURSUNOGLU; E-mail: sait.kursunoglu@agu.edu.tr
DOI: 10.1016/S1003-6326(20)65468-1

as a secondary source of metals due to the depletion of natural mineral resources in most industrialized countries [4]. The most important secondary sources of the zinc and lead are anodes, electric arc furnace dust, galvanizing plants, spent lead-acid batteries, pipes, solders, and dry cells, etc. The minerals of zinc and lead are naturally associated with each other. The mineralization of lead and zinc deposit is divided into three main categories: (1) sulphide ores, (2) mixed sulphide–oxide ores, and (3) non-sulphide ores, which formed hypogene or supergene weathering [5]. Zinc oxide ores, such as smithsonite ($ZnCO_3$), willemite (Zn_2SiO_4), hydrozincite ($2ZnCO_3·3Zn(OH)_2$), zincite (ZnO) and hemimorphite ($Zn_2SiO_3·H_2O$), are considered as important sources of zinc. Since oxide and carbonate minerals are generally amenable to atmospheric acid leaching, hydrometallurgical processes are preferred to treat such complex and low-grade source of metals containing finely disseminated lead and zinc, which are chemically similar. They are more attractive than pyrometallurgical processes as they are more environmentally friendly given the processes emit no hazardous dust and toxic gas, and require much lower capital for small scale operation [6,7].

The use of acidic reagents such as sulfuric acid solutions according to Eqs. (1)−(3) [8−18], alkaline reagents such as sodium hydroxide leaching of smithsonite [19], refractory hemimorphite zinc oxide ore [20], zinc silicate [21], low-grade oxide ore [22], smithsonite ores [23,24], Na_2EDTA solutions [25], leaching of smithsonite ore in ammonium chloride solution [26], leaching of nonsulfide zinc ore in ammonium carbonate solution [27], leaching of low-grade zinc oxide ore in ammonium hydroxide solution [28], leaching of low-grade zinc oxide ore in NH_3−NH_4Cl−H_2O solution [29], leaching of zinc silicate (hemimorphite) in ammoniacal solution [30], leaching of low grade zinc oxide ore in NH_4Cl−NH_3 solution [31], leaching of mixed sulfide–oxide zinc and lead ore in NH_3−$(NH_4)_2SO_4$ solution [32], leaching of zinc oxide ore in ammonia–ammonium sulfate solution [33], deep eutectic solvents [34], sulfosalicylic acid [35], zwitterionic reagent [36] has been reported to leach zinc from zinc or lead−zinc oxide and copper oxide ores. With the use of sulfuric acid solutions as lixiviant, the reports show that zinc in its oxide, silicate and carbonate forms is readily soluble according to the reactions shown in Eqs. (1)–(3). On the other hand, the lead sulphate is poorly soluble in sulfuric acid solution forcing lead to reprecipitate after its dissolution with the acid according to Eqs. (4) and (5) [17].

$$ZnO(s)+H_2SO_4(aq)\rightarrow ZnSO_4(aq)+H_2O(l),\ \Delta G_{298\ K}=-95.593\ \text{kJ/mol} \quad (1)$$

$$ZnCO_3(s)+H_2SO_4(aq)\rightarrow ZnSO_4(aq)+H_2O(l)+CO_2(g),\ \Delta G_{298\ K}=-78.855\ \text{kJ/mol} \quad (2)$$

$$Zn_2SiO_4(s)+2H_2SO_4(aq)\rightarrow 2ZnSO_4(aq)+Si(OH)_4(aq),\ \Delta G_{298\ K}=-134.570\ \text{kJ/mol} \quad (3)$$

$$PbCO_3(s)+H_2SO_4(aq)\rightarrow PbSO_4(s)+CO_2(g)+H_2O(l) \quad (4)$$

$$PbO(s)+H_2SO_4(aq)\rightarrow PbSO_4(s)+H_2O(l) \quad (5)$$

Iron is commonly present as an undesirable component of zinc tailings. During the leaching process, iron may dissolve along with zinc in sulfuric acid solution according to Eq. (6) [37]. This is undesirable because iron interferes with the zinc electrolysis process and therefore, it must be removed prior to the electrolysis step [38]. Iron may also cause some difficulties in the purification processes, especially where solvent extraction is used. In this case, the co-extraction of zinc with the iron species present in the solution can occur, thereby reducing the purification efficiency [39].

$$2FeO(OH)(s)+3H_2SO_4(aq)\rightarrow Fe_2(SO_4)_3(s)+4H_2O(l),\ \Delta G_{298\ K}=-164.731\ \text{kJ/mol} \quad (6)$$

In the present study, sulfuric acid and a mixture of sodium hydroxide and potassium sodium tartrate were explored for the separation of zinc and lead from the tailing. Although leaching zinc and lead from flotation tailings has not been previously reported, the present sequential leaching method is of interest in this study as it is able to bring about three different streams. This gives rise to the possibility of zinc and lead dissolution from the flotation tailing, leaving a considerable amount of iron in the final leach residue. Besides, mineralogical characterization of the leached residues, which is an essential step to examine the leaching process, was performed using XRD to understand the mineral dissolutions.

2 Experimental

The tailing sample was originated from Akkoyuncu Mining Co. in Yahyali-Kayseri, Turkey.

The sample was ground using a laboratory roll mill and analyzed by Mastersizer 2000 (Malvern). The mineralogical compositions were identified using Bruker D8 Discover (XRD) with Cu $K_{\alpha 1}$ (wavelength of 1.54060 Å) radiation source and calibrated with a silicon standard for alignment of 2θ=10°−70° radiation generated at 40 mA and 40 kV. The mineral phases were identified using Diffrac Suite EVA software equipped with the current ICDD PDF−2/Minerals database. The chemical composition of the sample was analyzed by Bureau Veritas Mineral Laboratory in Vancouver, Canada, via digestion and solution analysis using inductively coupled plasma mass spectroscopy (ICP-MS). Mineral assemblages in the sample were also analyzed by an optical microscope (ZEISS-Axiocam 506 color) to verify XRD results. A polished section was prepared using a standard epoxy resin. A total amounts of 30 mL of standard epoxy, 15 mL of epoxy hardener and 50 g of the sample were homogenously mixed and the mixture was placed in a cylindrical vessel. After 24 h of hardening the mixture, the hardened material was cut properly and each surface of the mixture (i.e. bottom and upper surfaces) was polished by silicon carbide waterproof abrasive paper. To confirm the XRD and polish section data before acid leaching, the representative sample was examined by field emission scanning electron microscopy (FE-SEM) coupled with energy-dispersive X-ray spectroscopy (EDX) (Zeiss GeminiSEM 300).

The leaching tests were performed in a 250 mL glass reactor. The leach slurry was mixed by a digital magnetic stirrer (MTOPS) at 400 r/min equipped with a temperature-controlled hot plate (MTOPS-MSDSM). In sulfuric acid leaching tests, the required volume of deionized water was transferred into the reactor and then heated to the desired temperature before adding ore sample to start the leaching process. 4 mol/L sulfuric acid was prepared by diluting analytical grade sulfuric acid (95%−97% in purity, Merck) in deionized water. pH was adjusted by a small addition of the 4 mol/L sulfuric acid using a syringe. The pH of the slurry was simultaneously controlled by pH meter equipped with IntelliCAL PHC 28101 and ORP probes (Hach, HQ40d). Figure 1 shows the experimental set-up. After the leaching experiment was finished, the slurry was filtered with Whatman 1 filter paper (70 mm in diameter) throughout vacuum filtration. The filtered residues were washed several times with deionized water. The filtrates were then subjected to atomic absorption spectroscopy (AAS, Thermo Scientific ICE 3300) for elemental analysis. The solid residue remained in the filter paper was dried in an oven at 105 °C for 24 h and analyzed by a X-ray fluorescence spectrometer (XRF) (Minipal 4 Panalytical). The changes in the mineralogical composition of the solid phase were identified by XRD analysis. In the alkaline leaching test, the remained solid residue was subjected to second step leaching using sodium hydroxide and potassium sodium tartrate solution. The filtrate was analyzed by AAS. The remained residue was dried and then analyzed by XRF to determine final residue content.

The electrowinning was conducted at ambient temperature using 50 mL of the electrolyte. A lead anode and aluminum cathode were used (each with surface area of 4 cm × 4 cm). The distance between anode and cathode was 5 cm. The solution was put in the 100 mL beaker and agitated with a magnetic

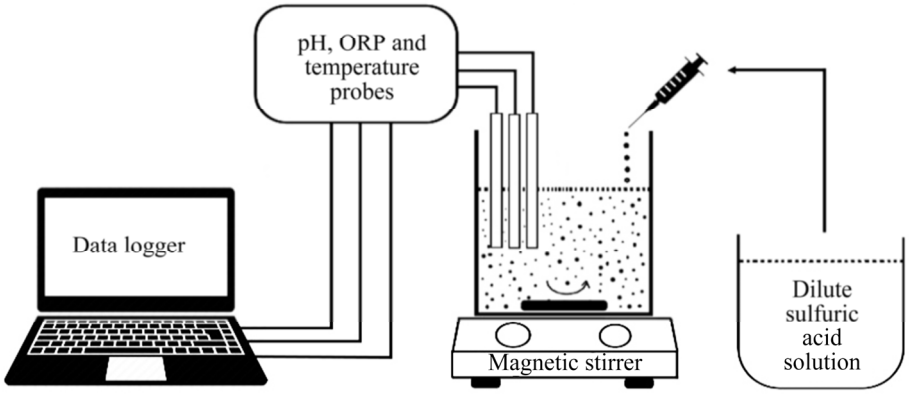

Fig. 1 Experimental set-up

stirrer (200 r/min). The cathodic current density was 0.7 A/cm^2. Electrolysis voltage was in a range of 4.5−4.7 V. pH of the electrolyte was arranged using sulfuric acid. The elemental composition of the cathode material was analyzed by XRF while phase composition was determined through XRD.

In the leaching tests, analytical-grade sulfuric acid (H_2SO_4, Merck), sodium hydroxide (NaOH, Merck) and potassium sodium tartrate ($KNaC_4H_4O_6·4H_2O$, Merck) were used. Deionized water was used for dilution when needed. In the acidic leaching tests, leaching time and stirring speed were kept constant at 2 h and 300 r/min, respectively. In the alkaline leaching, solid-to-liquid ratio, leaching time and stirring speed ratio were fixed at 10% (w/v), 2 h and 300 r/min, respectively. The leaching tests were duplicated to assess the reproducibility of the experimental results. The dissolution rate (D) was calculated according to the following equation:

$$D=\frac{C_L}{C_F}\times 100\% \quad (7)$$

where C_L and C_F are metal concentrations in the leach solution and feed, respectively.

3 Results and discussion

Figure 2 shows the particle size distribution of the ground sample. The results show that 90% of the sample was smaller than 146 μm. Table 1 gives the chemical compositions of the lead−zinc flotation tailing sample by ICP-MS. The XRD pattern is shown in Fig. 3. It is found that the major peaks were from smithsonite (card No. 08-0449), dolomite (card No. 36-0426), quartz (card No. 70-3755), calcite (card No. 05-0586) and goethite (card No. 81-0462). Minor peaks were also determined as corkite (card No. 15-0181) and cerussite (card No. 47-1734). Figure 4 shows the representative polished sections of the investigated sample. It is observed that the mineralizations of Pb, Zn, Ca and Fe were distinguishable on polished sections. For instance, Pb−Fe, Zn−Ca and Zn−Fe mineralizations present complex ore assemblages. In the meantime, Pb and Zn mineralizations were also hosted within the tailing. A representative SEM−EDX mapping result is given in Fig. 5. It is found that the contents of the metals from the XRD and optical microscope analysis were in good agreement with the findings of the SEM mapping analysis.

Table 1 Chemical composition of flotation tailing by ICP-MS (wt.%)

Pb	Zn	Fe	As	Ca	P
2.53	6.11	34.37	0.63	2.39	0.04
Mg	Ti	Al	Na	K	S
0.56	0.18	2.42	0.28	0.68	0.55

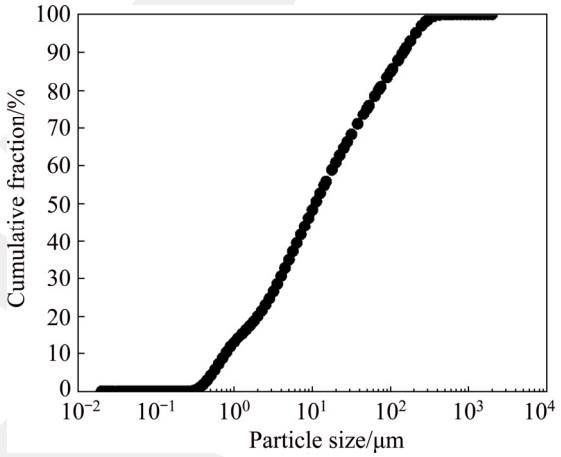

Fig. 2 Particle size distribution of ground sample

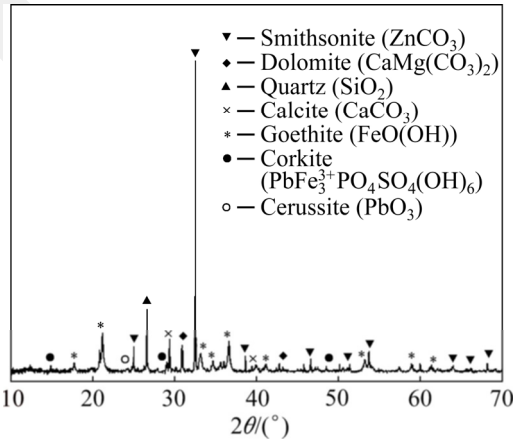

Fig. 3 XRD pattern of sample

3.1 Effect of leaching pH and solid-to-liquid (S/L) ratio on dissolution

Figure 6 shows the effects of pH and solid-to-liquid ratio on the dissolution of zinc, iron and lead from the flotation tailing at 25 °C for 2 h. It is shown that the zinc dissolution rate increased with decreasing pH of the leach slurry and solid-to-liquid ratio. The highest zinc dissolution achieved in this set of experiments was 72.5% at solid-to-liquid ratio of 10% and pH of 2. The iron co-dissolution

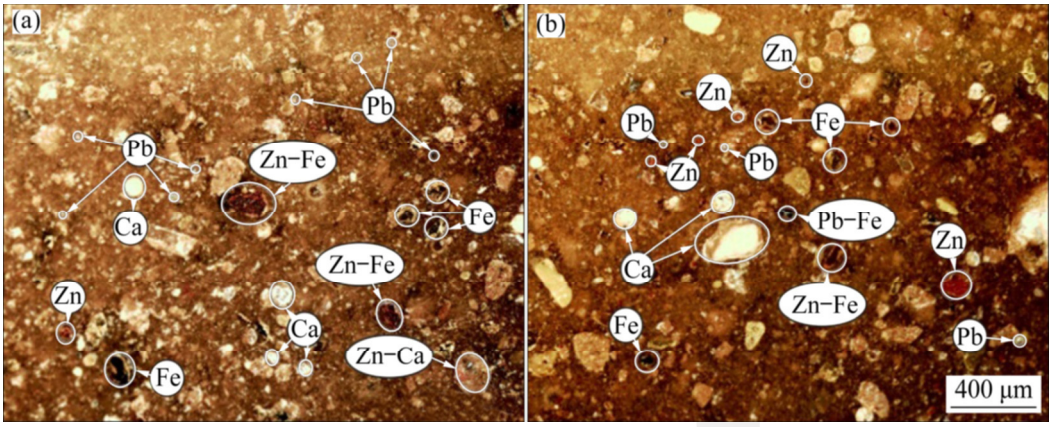

Fig. 4 Representative polished sections of sample

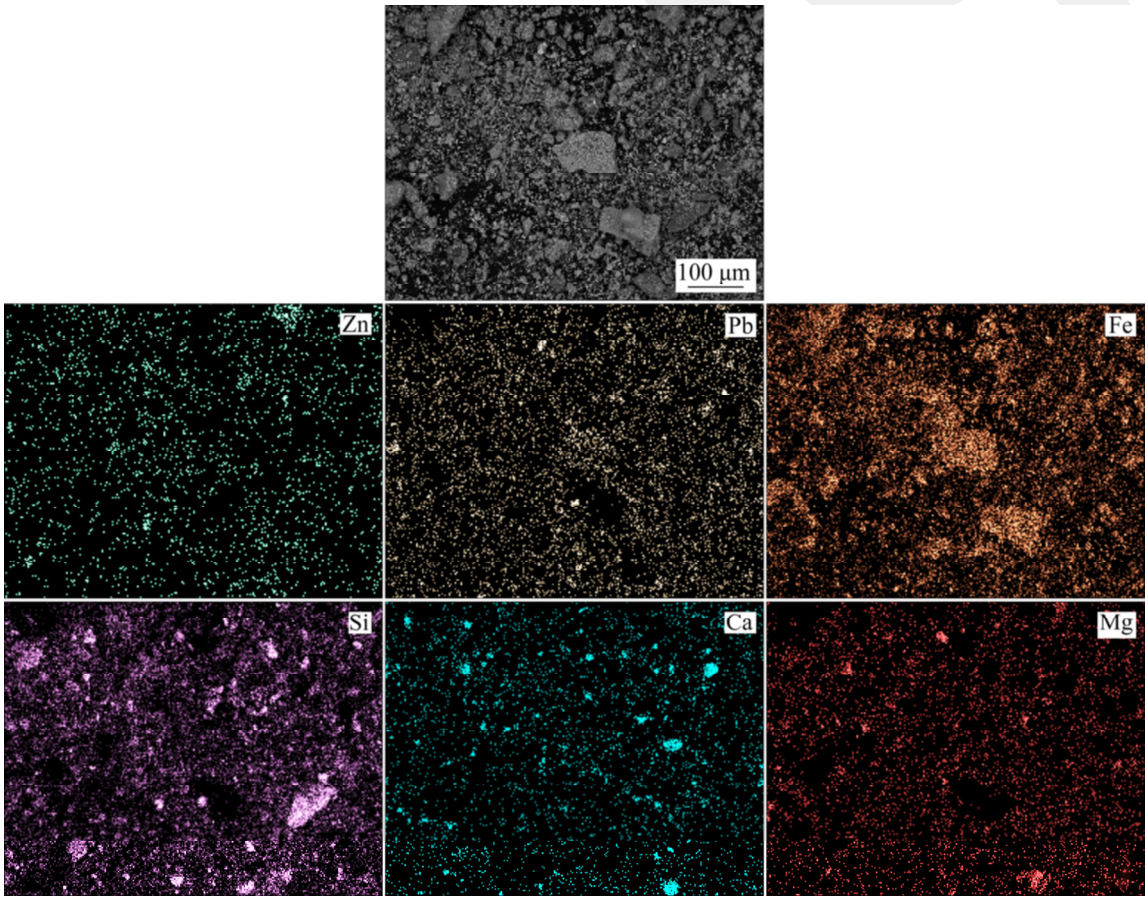

Fig. 5 SEM−EDX mapping of representative sample

under this condition, however, was only 0.7% while lead co-dissolution was insignificant, giving poor solubility of $PbSO_4$. The H^+ ions were easily diffused to the flotation tailing surface and subsequently dissolution rate increased at 10% of solid-to-liquid ratio. Under similar experimental conditions to those with different solid-to-liquid ratio of 20% and 30%, the zinc dissolution rate was decreased slightly as the pH of the leach slurry was kept constant. The highest zinc dissolutions, which were 69.4% and 66.1%, were achieved at pH 2. The results indicate the potential to separate zinc from iron and lead from the flotation tailing as the sulfuric acid leaching at pH 2 had good selectivity towards zinc leaving the other two metals in the residue. Compared to pH 3 and pH 4, the separation

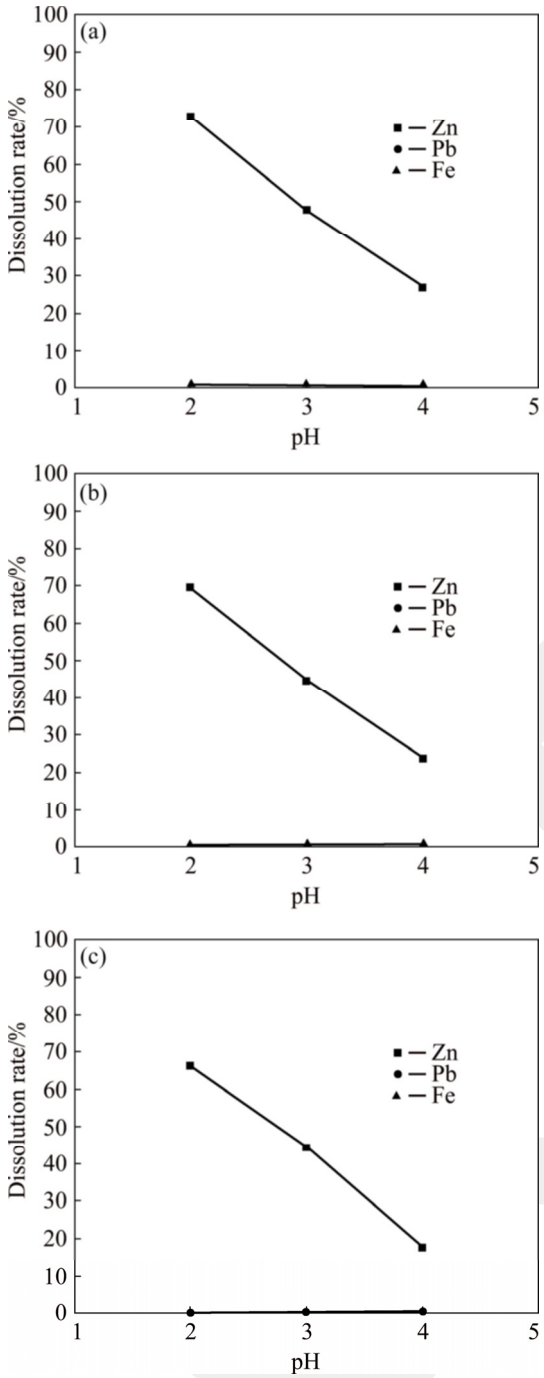

Fig. 6 Effect of pH on dissolution rate under different S/L ratio: (a) S/L ratio of 10%; (b) S/L ratio of 20%; (c) S/L ratio of 30%

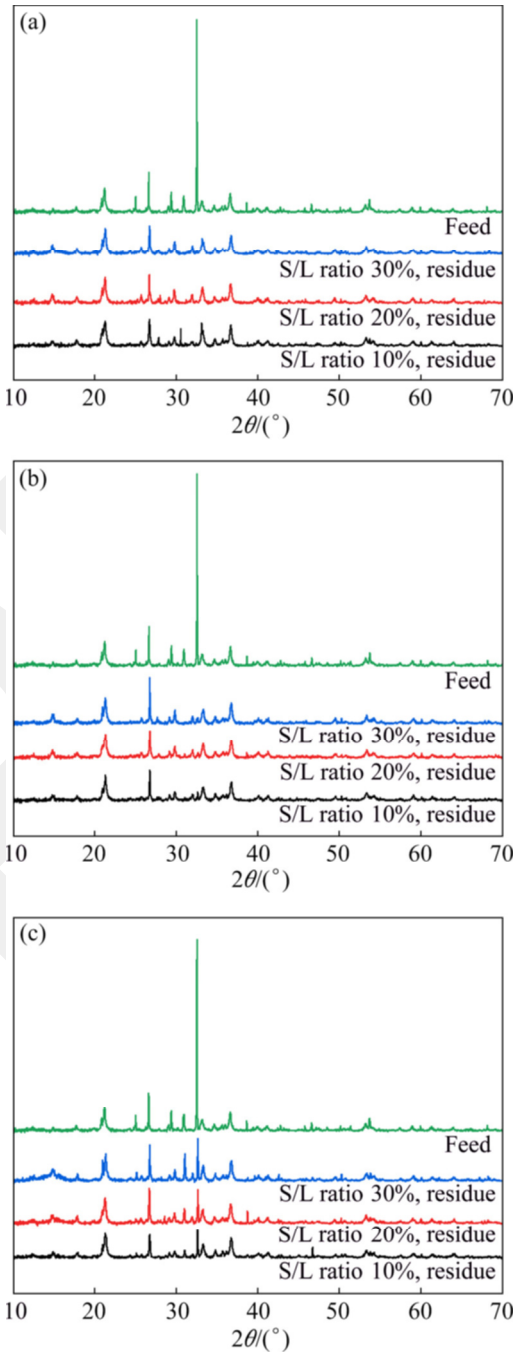

Fig. 7 XRD patterns of leach residue under different pH: (a) pH of 2; (b) pH of 3; (c) pH of 4

factor between zinc and iron was very high at pH 2. Hence, leaching experiments with pH of 2 and the solid-to-liquid ratio of 20% were selected in the further leaching experiments. Figure 7 shows the mineral phase changes during the leaching process. It is seen that smithsonite as a major peak significantly disappeared, which means that zinc was selectively extracted into the leach solution.

3.2 Effect of temperature on dissolution

Figure 8 shows the effect of temperature on the dissolution of zinc, lead and iron from the flotation tailing. From Fig. 8, the zinc dissolution rate was determined to be 82.3% at 40 °C, pH of 2 and solid-to-liquid ratio of 20% for 2 h while the iron and lead dissolution rates were less than 0.5%. When the leaching temperature was increased from 40 to 80 °C, there was no significant effect on zinc

dissolution. It is seen that the zinc oxide dissolution depended strongly on the pH of the solution. To decrease operational cost, the solid-to-liquid ratio of 20%, the temperature of 40 °C and pH of 2 were determined as the most appropriate conditions for the selective dissolution of zinc from the flotation tailing. The acid consumption under these optimum conditions was found to be 110.6 kg/t (dry ore). Figure 9 shows the pH and oxidation−reduction potential (ORP) changes of the leach slurry during the leaching process. In the first 20 min, ORP was significantly decreased in all leaching temperature and then stayed relatively constant. It is seen that the ORP changes were between 0.47 and 0.50 V, which means that zinc and iron were as form of Zn^{2+} and Fe^{2+} at pH of 2 (Fig. 10). It can also be seen that the only soluble iron species are ferrous iron (Fe^{2+}) and ferric iron (Fe^{3+}). Ferric iron is only stable at a limited area at lower pH-values and higher redox potential while ferrous iron is stable over a wider region at lower redox potential and higher pH values.

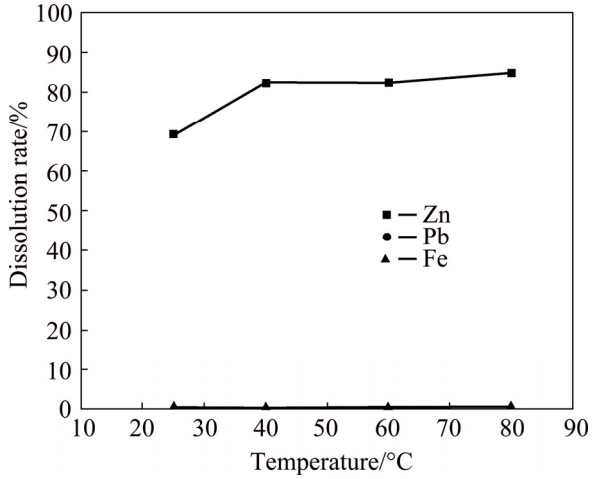

Fig. 8 Effect of temperature on dissolution rate (S/L ratio of 20%)

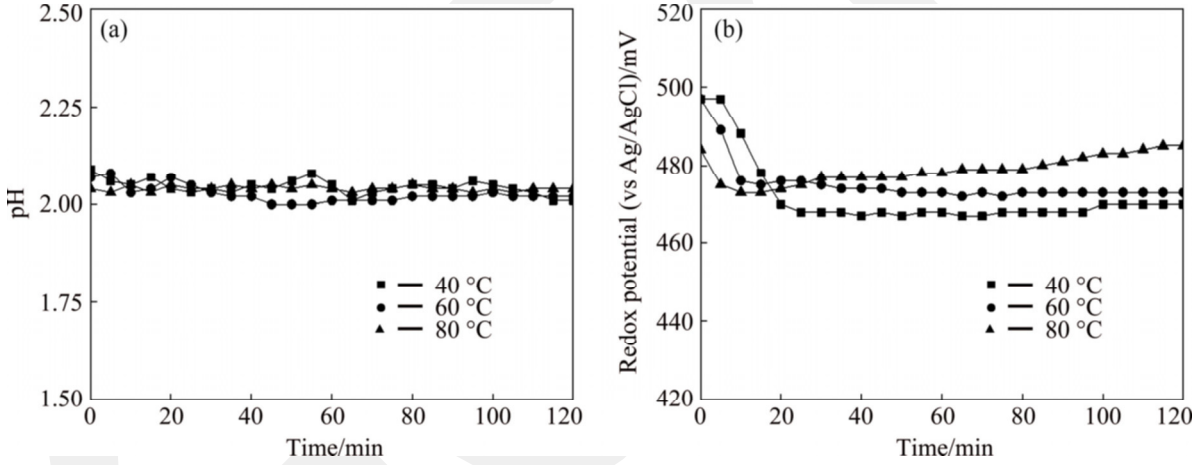

Fig. 9 pH (a) and ORP (b) changes of leach slurry (S/L ratio of 20%)

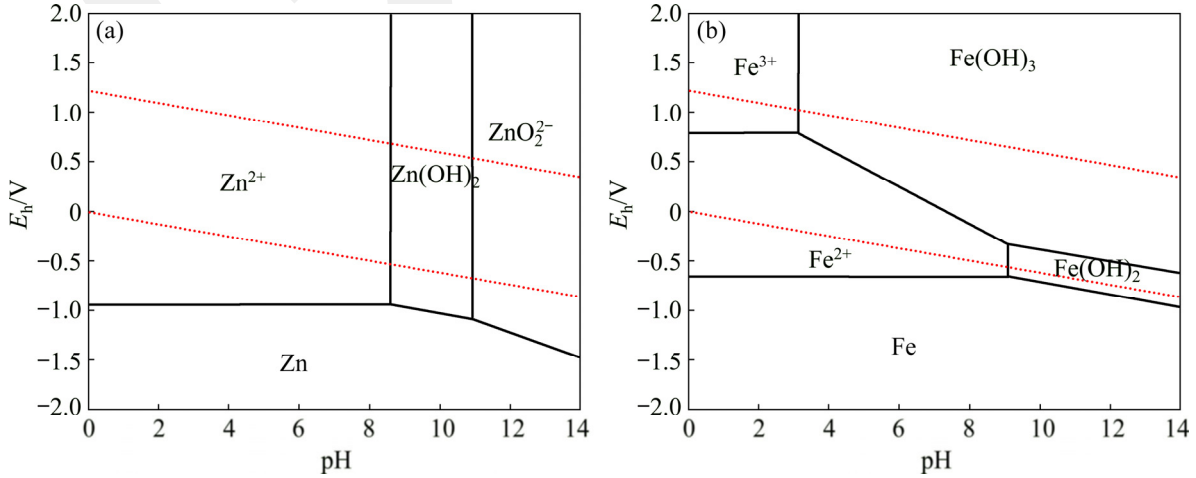

Fig. 10 E_h−pH diagram of Zn−H_2O (a) and Fe−H_2O (b) systems at 313.15 K (Molalities of Zn and Fe: 1×10^{-6} mol/kg, and pressure: 0.1 MPa)

3.3 Electrowinning of zinc from sulphate leach solution

The electrowinning of zinc was conducted by using the solution obtained directly after leaching at 40 °C and pH of 2. Electrowinning was performed at 25 °C for 30 min. No iron purification stage from the electrolyte required as the iron dissolution was less than 0.5% during the acidic leaching stage. When current passes to cause the decomposition of leach solution, the following reactions occur on the cathode and anode surface (Eqs. (8) and (9)). Metallic zinc was deposited at the cathode and stripped after sufficient metal buildup occurred. The deposited zinc was crystalline, gray in color, compact and fine-grained on the cathode surface. XRD and XRF analysis confirm that high-quality cathode product was obtained (Fig. 11).

The main cathodic reaction is

$$Zn^{++}(aq)+2e=Zn(s),\ \varphi^0=-0.76\ V \quad (8)$$

The following reaction occurs at the anode:

$$H_2O(l)=1/2O_2(g)+2H^+(aq)+2e,\ \varphi^0=-1.23\ V \quad (9)$$

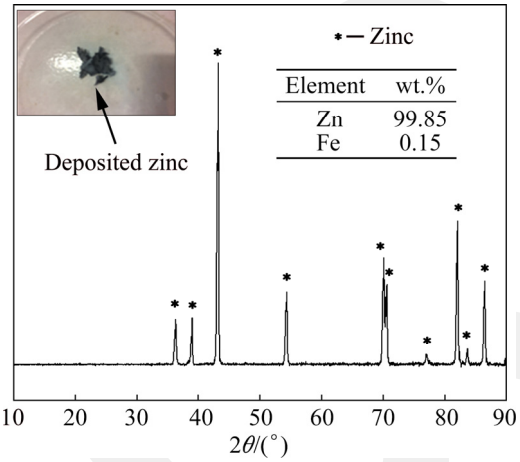

Fig. 11 XRD pattern of zinc collected at cathode

3.4 Effect of alkaline leaching on dissolution

The remained residue after the sulfuric acid leaching was fed to the second alkaline leaching unit. The chemical composition of the first stage leach residue is given in Table 2. The second stage alkaline leaching experiments using 50−150 g/L sodium hydroxide and a synergistic effect of potassium sodium tartrate in 150 g/L sodium hydroxide solution were conducted at 25 °C for 2 h. The stirring speed and solid-to-liquid ratio were 400 r/min and 10%, respectively. The zinc carbonate dissolution in sodium hydroxide solution is described by Eq. (10) [24], resulting in the zincate anion. After the first stage acidic leaching, lead sulphate precipitate was formed (Eqs. (4) and (5)). The lead sulphate dissolution took place in two-step according to Eqs. (11) and (12), resulting in the plumbite anion. BADANOIU et al [40] indicated that lead sulphate can dissolve easily in dilute sodium hydroxide solutions as well as at a low temperature. In this study, the use of milder conditions in the first step is preferred to minimize iron co-dissolution and to reduce the environmental impact and the operational cost of the process. Lead dissolution using milder conditions in the second stage was not attempted. So, iron dissolution with 50−150 g/L sodium hydroxide and 50−150 g/L potassium sodium tartrate and zinc dissolution with pH of 2 sulfuric acid solutions at 25 °C were compared. Sodium hydroxide has a strong oxidizing character and converts a part of PbO into PbO_2, which has a lower solubility in solutions. Besides, the compounds of Pb^{2+} convert into compounds of Pb^{4+}. Therefore, solid-to-liquid ratio of 10% was preferred in the alkaline leaching experiments.

$$ZnCO_3(s)+4OH^-(aq)\rightarrow Zn(OH)_4^-(aq)+CO_3^{2-}(aq) \quad (10)$$

$$PbSO_4(s)+2OH^-(aq)\rightarrow Pb(OH)_2(s)+SO_4^{2-}(aq) \quad (11)$$

$$Pb(OH)_2(s)+OH^-(aq)\rightarrow Pb(OH)_3^-(aq) \quad (12)$$

Table 2 Chemical composition of first stage leach residue by XRF (wt.%)

Al_2O_3	SiO_2	SO_3	K_2O	CaO
5.5	14	7.2	0.8	5.1
Fe_2O_3	ZnO	As_2O_3	Ag_2O	PbO
57.3	3.1	0.8	1.6	4.23

Figure 12 shows the dissolution rates of lead, zinc, and iron from the flotation tailing by the sequential leaching process using sodium hydroxide and potassium sodium tartrate at 25 °C in the second step. Using sodium hydroxide, the lead dissolution rate increased significantly until 10 g/L and then remained relatively constant. The lead dissolution rate was found to be 31.5%. The zinc and iron almost completely remained in the leach residue. In the case of potassium sodium tartrate, the lead dissolution rate was found to be 34.1% after 2 h leaching, whereas iron and zinc co-dissolution was not observed. Figure 13 shows

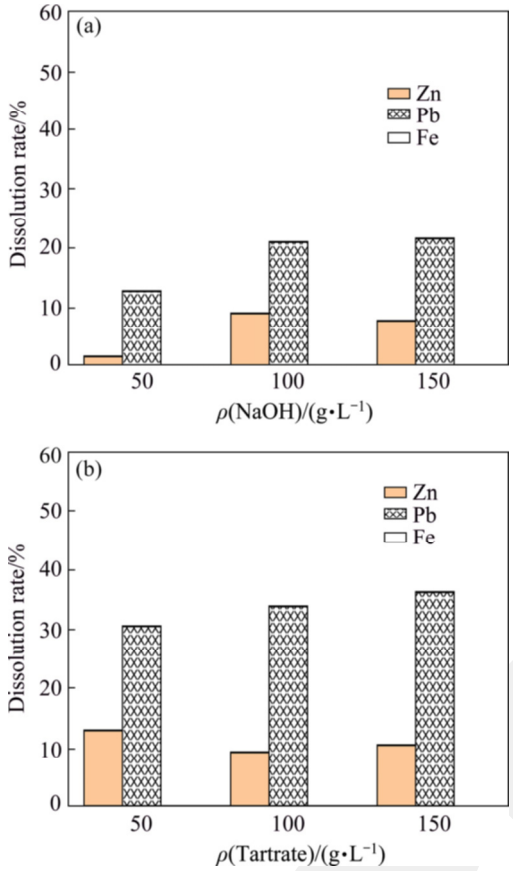

Fig. 12 Second stage alkaline leaching with sodium hydroxide (a) and potassium sodium tartrate in 150 g/L sodium hydroxide (b) at 25 °C and stirring speed of 400 r/min for 2 h

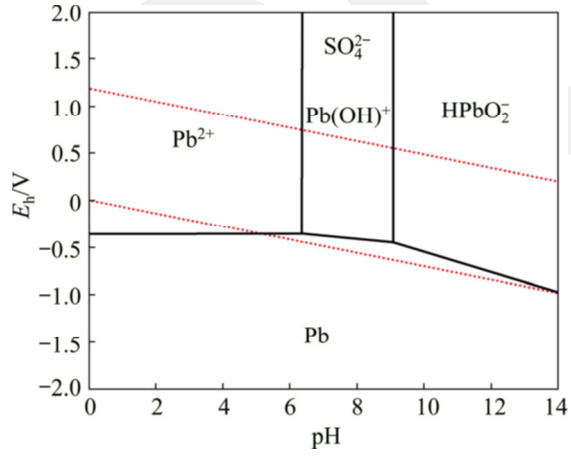

Fig. 13 E_h–pH diagram of Pb–H_2O system at 353.15 K (Molalities of Zn and Fe: 1×10^{-6} mol/kg, and pressure: 0.1 MPa)

E_h–pH diagrams of the Pb–H_2O system at 353.15 K. In alkaline media, $PbOH^+$ is only stable at a limited area at higher pH values and higher redox potential while Pb^{2+} is stable over a wider region at higher redox potential and lower pH values.

The second stage alkaline leaching was carried out by using 150 g/L sodium hydroxide + 150 g/L potassium sodium tartrate at different temperatures ranging from 40 to 80 °C for 2 h (Fig. 14). In this synergistic system, 62.7% dissolution of the remaining lead with 34.8% and 1.1% of zinc and iron co-dissolution, respectively, was achieved at 80 °C. FERRACIN et al [41] indicated that $PbSO_4$ and PbO dissolve in a mixture of sodium hydroxide and potassium sodium tartrate whereas Pb and PbO_2 are insoluble in this system. It is determined in the present study that the use of sulfuric acid at pH of 2 and 40 °C in the first leaching step was more advantageous given that it provides higher zinc dissolution and separation from lead and iron. In the second stage, more than 60% of lead was taken into the leach solution leaving appreciable iron in final residue. The final residue was analyzed by XRF (Table 3). The result indicates that more than 70% iron oxide remained in the residue, which was a saleable product for the iron−steel industry. To confirm the XRF analysis, the XRD analysis was carried out (Fig. 15). According to XRD analysis, the major peaks came from goethite and quartz mineral phases while minor peaks demonstrated smithsonite and cerussite. Therefore, the experimental results show that most zinc and lead

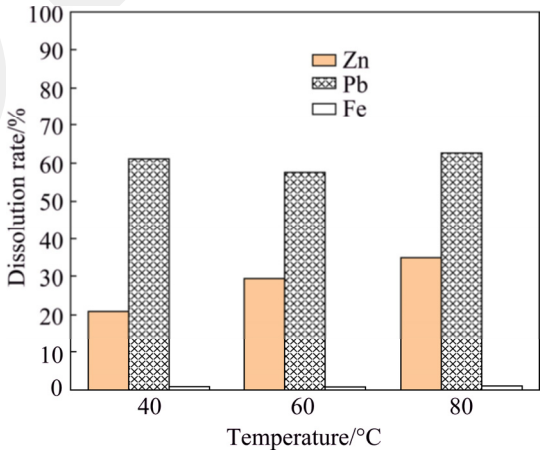

Fig. 14 Synergic effect of 150 g/L sodium hydroxide + 150 g/L potassium sodium tartrate system on dissolution at different temperatures

Table 3 Chemical composition of final residue (wt.%)

Al_2O_3	SiO_2	SO_3	K_2O	CaO
5.1	15	0.2	1.4	0.98
Fe_2O_3	ZnO	As_2O_3	Ag_2O	PbO
70.30	3.04	0.62	1.2	2.54

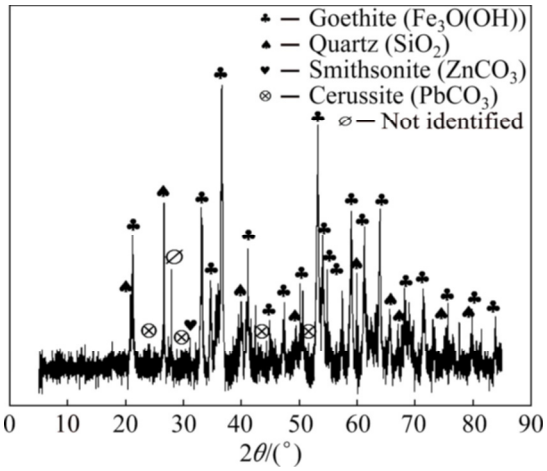

Fig. 15 XRD pattern of final residue

were depleted from the solid phase after sequential acidic and alkaline leaching while a considerable amount of iron remained in the solid phase.

4 Conclusions

(1) In the acidic leaching stage, 82.3% Zn was selectively taken into the leach solution, leaving a substantial amount of iron (99.5%) and lead (99.7%) in the leach residue.

(2) The sulfuric acid consumption under these optimum conditions was determined as 110.6 kg/t (dry tailing).

(3) There is no beneficial effect of leaching temperature on the zinc dissolution using sulfuric acid leaching.

(4) The electrowinning of sulphate leach solution showed that purity of deposited product on the cathode surface was determined as 99.8% Zn and 0.15% Fe.

(5) In the alkaline leaching stage, the dissolution of Pb increased slightly in the presence of potassium sodium tartrate. More than 60% of Pb dissolution was achieved when the leaching temperature increased from 40 to 80 °C.

(6) The final leach residue was subjected to XRD analysis and the results revealed that the major peaks originated from goethite and quartz.

(7) The XRF analysis demonstrated that the residue contained 70.3% Fe_2O_3.

(8) Based on the experimental results, zinc and lead were extracted from the flotation tailing, leaving a substantial amount of iron in the final residue.

Acknowledgments

This study was supported and financed by the European Union (E. U.) 1554 ERA-MIN2-Minteco Project and Scientific and Technological Research Council of Turkey 1555 (TUBITAK). The authors are thankful to the E. U. and TUBITAK (217M959) for financial support.

References

[1] ZHANG Y C, DENG J X, CHEN J, YU R B, XING X R. Leaching of zinc from calcined smithsonite using sodium hydroxide [J]. Hydrometallurgy, 2013, 131−132: 89−92.

[2] U.S. Geological Survey. Lead statistics and information [EB/OL]. https://minerals.usgs.gov/minerals/pubs/commodity/lead/index.html#mcs. 2018−11−18.

[3] U.S. Geological Survey. Zinc Statistics and Information [EB/OL]. https://minerals.usgs.gov/minerals/pubs/commodity/zinc/index.html#mcs. 2018−11−18.

[4] LUTANDULA M S, MALOBA B. Recovery of cobalt and copper through reprocessing of tailings from flotation of oxidised ores [J]. Journal of Environmental Chemical Engineering, 2013, 1: 1085−1090.

[5] GILG H A, BONI M, BALASSONE G, ALLEN C R, BANKS D, MOORE F. Marble hosted sulfide ores in the Angouran Zn–(Pb–Ag) deposit, NW Iran: Interaction of sedimentary brines with a metamorphic core complex [J]. Mineralium Deposita, 2006, 41(1): 1−16.

[6] JHA M K, KUMARI A, CHOUBEY P K, LEE J C, KUMAR V, JEONG J K. Leaching of lead from solder material of waste printed circuit boards (PCBs) [J]. Hydrometallurgy, 2012, 121−124: 28−34.

[7] SETHURAJAN M, HUGUENOT D, JAIN R, LENS P N L, HORN H A, FIGUEIREDO L H A, van HULLEBUSCH E D, Leaching and selective zinc recovery from acidic leachates of zinc metallurgical leach residues [J]. Journal of Hazardous Materials, 2017, 324(Part A): 71−82,

[8] TERRY B, MONHEMIUS A J. Acid dissolution of willemite ($(Zn,Mn)_2SiO_4$) and hemimorphite ($Zn_4Si_2O_7(OH)_2·H_2O$) [J]. Metallurgical Transactions B, 1983, 14: 335−346.

[9] BODAS M G. Hydrometallurgical treatment of zinc silicate ore from Thailand [J]. Hydrometallurgy, 1996, 40: 37−49.

[10] ABDEL-AAL E A, SHUKRY Z E. Application of quick leaching method to Egyptian zinc silicate ore [J]. Transactions of the Institution of Mining and Metallurgy (Section C: Mineral Processing and Extractive Metallurgy), 1997, 106: 89−90.

[11] ABDEL-AAL E A. Kinetics of sulfuric acid leaching of low-grade zinc silicate ore [J]. Hydrometallurgy, 2000, 55: 247−254.

[12] NAGIB S, INOUE K. Recovery of lead and zinc from fly ash generated from municipal incineration plants by means of acid and/or alkaline leaching [J]. Hydrometallurgy, 2000, 56: 269−292.

[13] ESPIARI S, RASHCHI F, SADRNEZHAAD S K.

Hydrometallurgical treatment of tailings with high zinc content [J]. Hydrometallurgy, 2006, 82: 54−62.

[14] SOUZA A D, PEINA P S, LIMA E V O, DASILVA C A, LEÃO V A. Kinetics of sulphuric acid leaching of a zinc silicate calcine [J]. Hydrometallurgy, 2007, 89: 337−345.

[15] SOUZA A D, PEINA P S, SANTOS F M F, DASILVA C A, LEÃO V A. Effect of iron in zinc silicate concentrate on leaching with sulphuric acid [J]. Hydrometallurgy, 2009, 95: 207−214.

[16] SAFARI V, AZARPEYMA G, RASHCHI F, MOSTOUFI N. A shrinking particle-shrinking core model for leaching of a zinc ore containing silica [J]. International Journal of Mineral Processing, 2009, 93: 79−83.

[17] MORADI S, MONHEMIUS A J. Mixed sulfide lead and zinc ores: Problems and solutions [J]. Minerals Engineering, 2011, 24: 1062−1076.

[18] ASADI T, AZIZI A, LEE J, JAHANI M. Leaching of zinc from a lead−zinc flotation tailing sample using ferric sulphate and sulfuric acid media [J]. Journal of Environmental Chemical Engineering, 2017, 5: 4769−4775.

[19] ZHAO Y, STANFORTH R. Production of Zn powder by alkaline treatment of smithsonite Zn−Pb ores [J]. Hydrometallurgy, 2000, 56: 237−249.

[20] CHEN A L, ZHAO Z W, JIA X J, LONG S, HUO G S, CHEN X Y. Alkaline leaching Zn and its concomitant metals from refractory hemimorphite zinc oxide ore [J]. Hydrometallurgy, 2009, 97: 228−232.

[21] SANTOS F M F, PEINA P S, PORCARO A, OLIVIERA V A, SILVA C A, LEAO V A. The kinetics of zinc silicate leaching in sodium hydroxide [J]. Hydrometallurgy, 2010, 102: 43−49.

[22] GHASEMI S M S, AZIZI A. Alkaline leaching of lead and zinc by sodium hydroxide: Kinetics modelling [J]. Journal of Materials Research and Technology, 2018, 7(2): 118−125.

[23] ZHANG Y C, DENG J X, CHEN J, YU R B, XING X R. A low-cost and large-scale synthesis of nano-zinc oxide from smithsonite [J]. Inorganic Chemistry Communications, 2014, 43: 138−141.

[24] EHSANI I, UCYILDIZ A, OBUT A. Leaching behaviour of zinc from a smithsonite ore in sodium hydroxide solutions [J]. Physicochemical Problems Miner Process, 2019, 55(2): 407−416.

[25] LIU Q, YANG S H, CHEN Y M, HE J, XUE H T. Selective recovery of lead from zinc oxide dust with alkaline Na_2EDTA solution [J]. Transactions of Nonferrous Metals Society of China, 2014, 24: 1179−1186.

[26] JU S H, TANG M T, YANG S H, LI Y N. Dissolution kinetics of smithsonite ore in ammonium chloride solution [J]. Hydrometallurgy, 2005, 80: 67−74.

[27] MOGHADDAM J, SARRAF-MAMOORY R, YAMINI Y, ABDOLLAHY M. Determination of the optimum conditions for the leaching of nonsulfide zinc ores (high-SiO_2) in ammonium carbonate media [J]. Industrial & Engineering Chemistry Research, 2005, 44: 8952−8958.

[28] FENG L Y, YANG X W, SHEN Q F, XU M L, JIN B J. Pelletizing and alkaline leaching of powdery low grade zinc oxide ores [J]. Hydrometallurgy, 2007, 89: 305−310.

[29] WANG R X, TANG M T, YANG S H, ZHAGN W H, TANG C B, HE J, YANG J G. Leaching kinetics of low grade zinc oxide ore in NH_3−NH_4Cl−H_2O system [J]. Journal of Central South University of Technology, 2008, 15: 679−683.

[30] DING Z Y, YIN Z L, HU H P, CHEN Q Y. Dissolution kinetics of zinc silicate (hemimorphite) in ammoniacal solution [J]. Hydrometallurgy, 2010, 104: 201−206.

[31] RAO S, YANG T Z, ZHANG D C, LIU W F, CHEN L, HAO Z D, XIAO Q K, WEN J F. Leaching of low grade zinc oxide ores in NH_4Cl–NH_3 solutions with nitrilotriacetic acid as complexing agents [J]. Hydrometallurgy, 2015, 158: 101−106.

[32] JIA N N, WANG H G, ZHANG M, GUO M. Selective and efficient extraction of zinc from mixed sulfide–oxide zinc and lead ore [J]. Mineral Processing and Extractive Metallurgy Review, 2016, 37(6): 418−426.

[33] YANG K, ZHANG L B, LV C, PENG J H, LI S W, MA A Y, CHEN W H, XIE F. Role of sodium citrate in leaching of low-grade and multiphase zinc oxide ore in ammonia–ammonium sulfate solution [J]. Hydrometallurgy, 2017, 169: 534−541.

[34] ZHU X L, XU C Y, TANG J, HUA Y X, ZHANG Q B, LIU H, WANG X, HUANG M T. Selective recovery of zinc from zinc oxide dust using choline chloride based deep eutectic solvents [J]. Transactions of Nonferrous Metals Society of China, 2019, 29: 2222−2228.

[35] DENG J S, WEN S M, YIN Q, WU D D, SUN Q W. Leaching of malachite using 5-sulfosalicylic acid [J]. Journal of the Taiwan Institute of Chemical Engineers, 2017, 71: 20−27.

[36] DENG J S, WEN S M, DENG J Y, WU D D. Extracting copper from copper oxide ore by a zwitterionic reagent and dissolution kinetics [J]. International Journal of Minerals, Metallurgy and Materials, 2015, 22: 241−248.

[37] TINDALL G P, MUIR D M. Effect of E_h on the rate and mechanism of the transformation of goethite into hematite in a high temperature acid leach process [J]. Hydrometallurgy, 1998, 47: 377−381.

[38] ISMAEL M R C, CARVALHO J M R. Iron recovery from sulphate leach liquors in zinc hydrometallurgy [J]. Minerals Engineering, 2003, 16: 31−39.

[39] BANZA A N, GOCK E, KONGOLO K. Base metals recovery from copper smelter slag by oxidizing leaching and solvent extraction [J]. Hydrometallurgy, 2002, 67: 63−69.

[40] BADANOIU G, BUZATU T, GHICA V G, BUZATU M, IACOB G, PETRESCU I M. Study of $PbSO_4$ solubilisation in NaOH solution, for the treatment of oxide-sulphate pastes obtained from dismembered lead-acid batteries [J]. UPB Scientific Bulletin, Series B: Chemistry and Materials Science, 2014, 76: 209−218.

[41] FERRACIN L C, CHA´CON-SANHUEZA A E, DAVOGLIO R A, ROCHA L O, CAFFEU D J, FONTANETTI A R, ROCHA-FILHO R C, BIAGGIO S R, BOCCHI N. Lead recovery from a typical Brazilian sludge of exhausted lead-acid batteries using an electro-hydrometallurgical process [J]. Hydrometallurgy, 2002, 65: 137−144.

采用硫酸浸出和添加酒石酸钾钠的氢氧化钠浸出从 Yahyali 非硫化浮选尾矿中回收锌和铅

Sait KURSUNOGLU[1], Soner TOP[1], Muammer KAYA[2]

1. Department of Materials Science & Nanotechnology Engineering, Abdullah Gul University, Kayseri 38100, Turkey;
2. Division of Mineral Processing, Department of Mining Engineering,
Eskisehir Osmangazi University, Eskisehir 26480, Turkey

摘　要：采用硫酸浸出和添加酒石酸钾钠的氢氧化钠浸出从 Yahyali 非硫化浮选尾矿中回收锌和铅。在酸浸阶段，研究 pH 值、固液比和温度对尾矿中锌溶出的影响。在 pH 值为 2、温度为 40 °C、固液比为 20%、浸出时间为 2 h 的条件下，锌的溶出率达到 82.3%，而铁和铅的溶出率低于 0.5%。硫酸消耗量为 110.6 kg/t(干尾矿)。浸出温度对尾矿中锌的溶出无有益的影响。酸浸液的电积试验结果表明，阴极产物含 99.8%的 Zn 和 0.15%的 Fe。在碱浸阶段，添加酒石酸钾钠时铅的溶出率略有增加，浸出温度从 40 °C 升高到 80 °C 时，超过 60%的 Pb 进入浸出液中。利用 XRD 和 XRF 分析最终的浸出渣。XRD 分析结果表明，主要衍射峰来自针铁矿和石英，次要衍射峰属于菱锌矿和白铅矿。XRF 分析结果显示，浸出渣含有 70.3%的氧化铁。基于顺序浸出实验结果，浸选尾矿中的锌和铅可以被很好地浸出，而大量的铁留在浸出渣中。

关键词：锌；铅；浮选尾矿；顺序浸出

(Edited by Bing YANG)